Y. S. Kim
Graduate Research Assistant,
School of Civil and Environmental Engineering.

G. A. Kardomateas
Professor,
School of Aerospace Engineering,
Fellow ASME

A. Zureick
Professor,
School of Civil and Environmental Engineering.

Georgia Institute of Technology,
Atlanta, GA 30332

Buckling of Thick Orthotropic Cylindrical Shells Under Torsion

A three-dimensional elasticity solution to the problem of buckling of orthotropic cylindrical shells under torsion is presented. A mixed form of the Galerkin method with a series of Legendre polynomials in the thickness coordinate has been applied to solve the governing differential equations. The accuracy of existing shell theory solutions has been assessed through a comparison study for both isotropic and orthotropic cylinders. For isotropic cylinders the solutions based on the Donnell shell theory were found to predict nonconservative values for the critical loads. As the circumferential wave numbers increase, shell theory solutions provide more accurate values. For orthotropic cylinders, the classical shell theory predicts much higher critical loads for a relatively short and thick cylinder, while the shear deformation theories provide results reasonably close to the elasticity solutions. Detailed data are also presented for the critical torsional loads over a wide range of length ratios and radius ratios for isotropic, glass/epoxy, and graphite/epoxy cylinders.

Introduction

Composite materials have gained widespread usage in structural applications because of their unique properties such as high strength-to-weight ratio and corrosion resistance. Both plate and shell structural laminated composite configurations have found technical applications in aircraft and marine industries. In particular, circular cylindrical shells can be used as primary load-carrying members in many industrial applications (e.g., torsion bars in automotive suspension components) and under a variety of loading configurations. It is therefore of great technical importance when designing lightweight cylindrical shells to clarify the elastic stability characteristics.

The review articles by Ambartsumian (1962), Bert and Francis (1974), Tennyson (1975), and Simitses (1986, 1996) provided detailed accounts of the evolution of the active research dealing with composite cylindrical shells. Some of works summarized in those articles employed classical shell theories and the others did refined theories including shear deformation effects. However, shell theories and formulations, be they classical or refined, are inherently approximate since they are based directly upon initial assumptions and hypotheses. Furthermore, existence of different shell theories underscores the need for elasticity solutions to use as benchmarks for comparison of predictions from the various approximate methods.

Recently, several three-dimensional elasticity-based buckling solutions have become available in the cylindrical shell literature. Babich and Kilin (1985) investigated on axisymmetric but three-dimensional form of stability loss of a three-layered orthotropic cylindrical shell under axial compression. Kardomateas (1993a) dealt with the problem of an orthotropic cylinder under uniform external pressure on the basis of the "ring assumption," in that the prebuckling stress and displacement field was axisymmetric, and the buckling modes were assumed to be two-dimensional. In a further study (Kardomateas and Chung, 1994), this ring assumption was relaxed so that a nonzero axial displacement and a full dependence of buckling modes on the three coordinates were assumed. A more thorough investigation of the thickness effect was conducted by Kardomateas (1993b) for the case of a transversely isotropic thick cylindrical shell under axial compression. In this work, he presented a closed-form solution in terms of Bessel functions.

In more recent studies, Kardomateas (1995, 1996) considered the problem of buckling of orthotropic cylindrical shells under axial compression in one case and combined axial compression and external pressure in another case. These works included comprehensive studies of the performance of shell formulations by Donnell (1933), Flügge (1960), Danielson and Simmonds (1969), and Timoshenko and Gere (1961). Other three-dimensional elasticity results that dealt with orthotropic and cross-ply laminated cylinders and cylindrical panels under combined axial compression and uniform external pressure were presented by Soldatos and Ye (1994) and Ye and Soldatos (1995). These studies provided elasticity solutions by using the successive approximation method.

An investigation of the literature presented above revealed that little information is available on the three-dimensional elasticity-based buckling analysis of orthotropic cylindrical shells under torsion. Therefore, in the current study, an orthotropic cylindrical shell with fixed ends, subjected to torsion, is studied. Employing cylindrical coordinates r, θ, and z (see Fig. 1), the nonlinear three-dimensional theory of elasticity is appropriately formulated following Kardomateas (1993a). This problem is more complicated than the pure external pressure or axial compression one due to the coupled torsional displacement modes of the first-order field (non-separable function of θ and z). Applying displacements at the prebuckling state, buckling equations are reduced to three linear homogenous differential equations in terms of the displacements of the perturbed state. A mixed-form Galerkin procedure is employed to solve these equations and to find numerical values for the critical loads. After comparing the results of this study with the ones from shell theories for a variety of example problems, an extensive parametric study of both isotropic and orthotropic cylinders is performed.

Formulation

For a homogeneous orthotropic cylindrical shell occupying a region in the three-dimensional Euclidean space referred to a cylindrical coordinate system (r, θ, z) in which the z-axis coincides with the longitudinal axis of the shell as shown in Fig. 1, the stress-strain relationships can be expressed in the form

Contributed by the Applied Mechanics Division of THE AMERICAN SOCIETY OF MECHANICAL ENGINEERS for publication in the ASME JOURNAL OF APPLIED MECHANICS.

Discussion on the paper should be addressed to the Technical Editor, Professor Lewis T. Wheeler, Department of Mechanical Engineering, University of Houston, Houston, TX 77204-4792, and will be accepted until four months after final publication of the paper itself in the ASME JOURNAL OF APPLIED MECHANICS.

Manuscript received by the ASME Applied Mechanics Division, Feb. 10, 1998; final revision, May 12, 1998. Associate Technical Editor: S. Kyriakides.

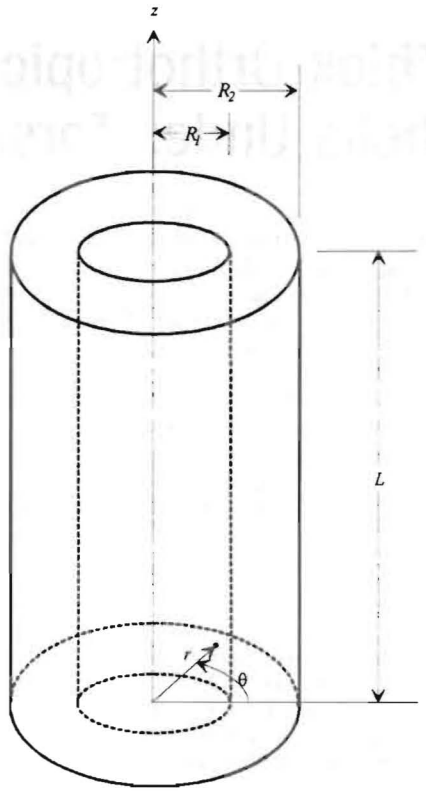

Fig. 1 Dimensions and coordinates for a cylindrical shell

$$\begin{bmatrix} \sigma_{rr} \\ \sigma_{\theta\theta} \\ \sigma_{zz} \\ \tau_{\theta z} \\ \tau_{rz} \\ \tau_{r\theta} \end{bmatrix} = \begin{bmatrix} c_{11} & c_{12} & c_{13} & 0 & 0 & 0 \\ c_{12} & c_{22} & c_{23} & 0 & 0 & 0 \\ c_{13} & c_{23} & c_{33} & 0 & 0 & 0 \\ 0 & 0 & 0 & c_{44} & 0 & 0 \\ 0 & 0 & 0 & 0 & c_{55} & 0 \\ 0 & 0 & 0 & 0 & 0 & c_{66} \end{bmatrix} \begin{bmatrix} \epsilon_{rr} \\ \epsilon_{\theta\theta} \\ \epsilon_{zz} \\ \gamma_{\theta z} \\ \gamma_{rz} \\ \gamma_{r\theta} \end{bmatrix}, \quad (1)$$

where c_{ij} are the stiffness coefficients and ϵ_{rr}, $\epsilon_{\theta\theta}$, ϵ_{zz}, $\gamma_{r\theta}$, γ_{rz}, $\gamma_{\theta z}$ are the engineering strains defined by the following nonlinear kinematic equations:

$$\epsilon_{rr} = u_{,r} + \tfrac{1}{2}(u_{,r}^2 + v_{,r}^2 + w_{,r}^2), \quad (2a)$$

$$\epsilon_{\theta\theta} = \frac{v_{,\theta}}{r} + \frac{u}{r} + \frac{1}{2r^2}[(u_{,\theta} - v)^2 + (v_{,\theta} + u)^2 + (w_{,\theta})^2], \quad (2b)$$

$$\epsilon_{zz} = w_{,z} + \tfrac{1}{2}(u_{,z}^2 + v_{,z}^2 + w_{,z}^2), \quad (2c)$$

$$\gamma_{r\theta} = \frac{u_{,\theta}}{r} + v_{,r} - \frac{v}{r} + \frac{1}{r}[u_{,r}(u_{,\theta} - v) + v_{,r}(v_{,\theta} + u) + w_{,r}(w_{,\theta})], \quad (2d)$$

$$\gamma_{rz} = u_{,z} + w_{,r} + (u_{,r}u_{,z} + v_{,r}v_{,z} + w_{,r}w_{,z}), \quad (2e)$$

$$\gamma_{\theta z} = v_{,z} + \frac{w_{,\theta}}{r} + \frac{1}{r}[u_{,z}(u_{,\theta} - v) + v_{,z}(v_{,\theta} + u) + w_{,z}(w_{,\theta})]. \quad (2f)$$

In the general stability theory of elastic solids, it is known that at the critical load there are two possible infinitely close positions of equilibrium. Denoting u_0, v_0, w_0 as the r, θ, and z components of displacement corresponding to the primary position, the displacements in the perturbed position are denoted by

$$u = u_0 + \alpha u_1(r, \theta, z); \quad v = v_0 + \alpha v_1(r, \theta, z);$$
$$w = w_0 + \alpha w_1(r, \theta, z), \quad (3)$$

where α is an infinitesimally small quantity. Here, $\alpha u_1(r, \theta, z)$, $\alpha v_1(r, \theta, z)$, and $\alpha w_1(r, \theta, z)$ are displacements that points of the body must undergo to shift them from their initial equilibrium position to their new equilibrium position. The functions $u_1(r, \theta, z)$, $v_1(r, \theta, z)$, and $w_1(r, \theta, z)$ are assumed finite and α is independent of r, θ, and z.

Substituting (3) into (2) results in the following equations for the strain components in the perturbed state:

$$\epsilon_{ij} = \epsilon_{ij}^0 + \alpha\epsilon_{ij}' + \alpha^2\epsilon_{ij}'', \quad (4)$$

where ϵ_{ij}^0 are values of the strain components in the initial position of equilibrium; ϵ_{ij}' are strain quantities that depend on derivatives of both u_0, v_0, w_0 and u_1, v_1, w_1; and ϵ_{ij}'' are parameters that depend only on derivatives of u_1, v_1, w_1 and contain only quadratic terms. Substitution of (4) into (1) yields

$$\sigma_{ij} = \sigma_{ij}^0 + \alpha\sigma_{ij}' + \alpha^2\sigma_{ij}'', \quad (5)$$

where σ_{ij}^0, σ_{ij}', and σ_{ij}'' can be expressed in the form of (1) by replacing ϵ_{ij} by ϵ_{ij}^0, ϵ_{ij}', and ϵ_{ij}'', respectively.

From three-dimensional elasticity theory (Ciarlet, 1988), the equations of equilibrium are expressed in terms of the second Piola-Kirchhoff stress tensor Σ in the form

$$\text{div}(\Sigma \cdot F^T) = 0, \quad (6)$$

where F is the deformation gradient defined by

$$F = I + (\text{grad } V)^T, \quad (7)$$

where V is the displacement vector and I is the identity tensor. The linear strains are also introduced as

$$e_{rr} = u_{,r}, \quad e_{\theta\theta} = \frac{v_{,\theta}}{r} + \frac{u}{r}, \quad e_{zz} = w_{,z}, \quad (8a)$$

$$e_{r\theta} = \frac{u_{,\theta}}{r} + v_{,r} - \frac{v}{r}, \quad e_{rz} = u_{,z} + w_{,r}, \quad e_{\theta z} = v_{,z} + \frac{w_{,\theta}}{r}, \quad (8b)$$

and the linear rotations as

$$2\omega_r = \frac{w_{,\theta}}{r} - v_{,z}, \quad 2\omega_\theta = u_{,z} - w_{,r}, \quad 2\omega_z = v_{,r} + \frac{v}{r} - \frac{u_{,\theta}}{r}. \quad (8c)$$

Following Kardomateas (1993a), the following buckling equations govern the first-order field:

$$\frac{\partial}{\partial r}(\sigma_{rr}' - \tau_{r\theta}^0\omega_z' + \tau_{rz}^0\omega_\theta') + \frac{1}{r}\frac{\partial}{\partial\theta}(\tau_{r\theta}' - \sigma_{\theta\theta}^0\omega_z' + \tau_{\theta z}^0\omega_\theta') + \frac{\partial}{\partial z}(\tau_{rz}' - \tau_{\theta z}^0\omega_z' + \sigma_{zz}^0\omega_\theta') + \frac{1}{r}(\sigma_{rr}' - \sigma_{\theta\theta}' + \tau_{rz}^0\omega_\theta' + \tau_{\theta z}^0\omega_r' - 2\tau_{r\theta}^0\omega_z') = 0, \quad (9a)$$

$$\frac{\partial}{\partial r}(\tau_{r\theta}' + \sigma_{rr}^0\omega_z' + \tau_{rz}^0\omega_r') + \frac{1}{r}\frac{\partial}{\partial\theta}(\sigma_{\theta\theta}' + \tau_{r\theta}^0\omega_z' - \tau_{\theta z}^0\omega_r') + \frac{\partial}{\partial z}(\tau_{\theta z}' + \tau_{rz}^0\omega_z' - \sigma_{zz}^0\omega_r') + \frac{1}{r}(2\tau_{r\theta}' + \sigma_{rr}^0\omega_z' - \sigma_{\theta\theta}^0\omega_z' + \tau_{\theta z}^0\omega_\theta' - \tau_{rz}^0\omega_r') = 0, \quad (9b)$$

$$\frac{\partial}{\partial r}(\tau'_{r} - \sigma^0_{rr}\omega'_\theta + \tau^0_{r\theta}\omega'_r) + \frac{1}{r}\frac{\partial}{\partial\theta}(\tau'_{\theta z} - \tau^0_{r\theta}\omega'_\theta + \sigma^0_{\theta\theta}\omega'_r)$$

$$+ \frac{\partial}{\partial z}(\sigma'_{zz} - \tau^0_{rz}\omega'_\theta + \tau^0_{\theta z}\omega'_r)$$

$$+ \frac{1}{r}(\tau'_{rz} - \sigma^0_{rr}\omega'_\theta + \tau^0_{r\theta}\omega'_r) = 0. \quad (9c)$$

The boundary conditions associated with (6) can be expressed as

$$(F\cdot\Sigma^T)\cdot\hat{N} = t(V), \quad (10)$$

where t is the traction vector on the surface having an outward unit normal $\hat{N} = (\hat{l}, \hat{m}, \hat{n})$ before deformation. Traction vector t depends on the displacement field $V = (u, v, w)$. Again, following Kardomateas (1993a), the following boundary conditions at the lateral and end surfaces are obtained:

$$(\sigma'_{rr} - \tau^0_{r\theta}\omega'_z + \tau^0_{rz}\omega'_\theta)\hat{l} + (\tau'_{r\theta} - \sigma^0_{\theta\theta}\omega'_z + \tau^0_{\theta z}\omega'_\theta)\hat{m}$$

$$+ (\tau'_{rz} - \tau^0_{\theta z}\omega'_z + \sigma^0_{zz}\omega'_\theta)\hat{n} = 0, \quad (11a)$$

$$(\tau'_{r\theta} + \sigma^0_{rr}\omega'_z + \tau^0_{rz}\omega'_r)\hat{l} + (\sigma'_{\theta\theta} + \tau^0_{r\theta}\omega'_z - \tau^0_{\theta z}\omega'_r)\hat{m}$$

$$+ (\tau'_{\theta z} + \tau^0_{rz}\omega'_z - \sigma^0_{zz}\omega'_r)\hat{n} = 0, \quad (11b)$$

$$(\sigma'_{rr} - \tau^0_{r\theta}\omega'_z + \tau^0_{rz}\omega'_\theta)\hat{l} + (\tau'_{r\theta} - \sigma^0_{\theta\theta}\omega'_z + \tau^0_{\theta z}\omega'_\theta)\hat{m}$$

$$+ (\tau'_{rz} - \tau^0_{\theta z}\omega'_z + \sigma^0_{zz}\omega'_\theta)\hat{n} = 0. \quad (11c)$$

In an orthotropic cylindrical shell subjected to pure torsion, the cross section of the cylinder simply rotates about the longitudinal axis, and thus similar to the case of isotropy, the displacements at the initial position are expressed in the form:

$$u_0 = w_0 = 0; \quad v_0 = \frac{M}{C}rz, \quad (12)$$

where M is the torque at both ends and C is the torsional rigidity of the cylinder, defined as $C = c_{44}\pi(R_2^4 - R_1^4)/2$, where R_1 and R_2 are inner and outer radius, respectively.

Using Eqs. (1) and (8), we obtain the strain components at the prebuckling state,

$$e^0_{rr} = e^0_{\theta\theta} = e^0_{zz} = e^0_{r\theta} = e^0_{rz} = 0, \quad e^0_{\theta z} = \frac{M}{C}r, \quad (13)$$

and the stress components,

$$\sigma^0_{rr} = \sigma^0_{\theta\theta} = \sigma^0_{zz} = \tau^0_{r\theta} = \tau^0_{rz} = 0, \quad \tau^0_{\theta z} = \frac{c_{44}M}{C}r. \quad (14)$$

Substitution of (14) and the expressions for σ'_{ij} and ω'_i in terms of the displacements from (1) and (8) transforms the buckling Eqs. (9) into the following system of three linear homogenous partial differential equations with three unknown displacement functions u_1, v_1, and w_1:

$$c_{11}u_{1,rr} + c_{11}\frac{u_{1,r}}{r} + c_{66}\frac{u_{1,\theta\theta}}{r^2} + c_{55}u_{1,zz} - c_{22}\frac{u_1}{r^2} + 2\bar{M}u_{1,\theta z}$$

$$+ (c_{12} + c_{66})\frac{v_{1,r\theta}}{r} - (c_{22} + c_{66})\frac{v_{1,\theta}}{r^2} - \bar{M}(rv_{1,rz} + 2v_{1,z})$$

$$+ (c_{13} + c_{55})w_{1,rz} + (c_{13} - c_{23})\frac{w_{1,z}}{r}$$

$$- \bar{M}\left(w_{1,r\theta} - \frac{w_{1,\theta}}{r}\right) = 0, \quad (15a)$$

$$(c_{12} + c_{66})\frac{u_{1,r\theta}}{r} + (c_{22} + c_{66})\frac{u_{1,\theta}}{r^2} + \bar{M}u_{1,z} + c_{66}v_{1,rr} + c_{66}\frac{v_{1,r}}{r}$$

$$+ c_{22}\frac{v_{1,\theta\theta}}{r^2} + c_{44}v_{1,zz} - c_{66}\frac{v_1}{r^2} + \bar{M}v_{1,\theta z} + (c_{23} + c_{44})\frac{w_{1,\theta z}}{r}$$

$$- \bar{M}\left(w_{1,r} + \frac{w_{1,\theta\theta}}{r}\right) = 0, \quad (15b)$$

$$(c_{13} + c_{55})u_{1,rz} + (c_{23} + c_{55})\frac{u_{1,z}}{r} + (c_{23} + c_{44})\frac{v_{1,\theta z}}{r} - \bar{M}rv_{1,zz}$$

$$+ c_{55}w_{1,rr} + c_{55}\frac{w_{1,r}}{r} + c_{44}\frac{w_{1,\theta\theta}}{r^2} + c_{33}w_{1,zz} + \bar{M}w_{1,\theta z} = 0. \quad (15c)$$

In the same manner, three homogeneous boundary conditions can be obtained from (11) for the lateral surfaces for $\hat{m} = \hat{n} = 0$ and $\hat{l} = \pm 1$:

$$c_{11}u_{1,r} + c_{12}\frac{u_1}{r} + c_{12}\frac{v_{1,\theta}}{r} + c_{13}w_{1,z} = 0 \text{ at } r = R_1, R_2, \quad (16a)$$

$$c_{66}\frac{u_{1,\theta}}{r} + c_{66}v_{1,r} - c_{66}\frac{v_1}{r} = 0 \text{ at } r = R_1, R_2, \quad (16b)$$

$$c_{55}u_{1,z} + c_{55}w_{1,r} = 0 \text{ at } r = R_1, R_2, \quad (16c)$$

where $\bar{M} = Mc_{44}/2C$.

There is a substantial difference between Eqs. (15) and those obtained by Kardomateas (1993a, 1995) for the case of buckling of an orthotropic cylindrical shell subjected to lateral or axial compression. This difference is that in the same equation we encounter both odd and even orders of derivatives of a displacement with respect to the same independent variable. This prevents one from reducing (15) to ordinary differential equations by applying a separable form of displacement functions as in the external pressure or the axial compression loading case. Therefore, a solution procedure using the Galerkin method is employed in this study.

For convenience, equations (15) and (16) are rewritten in the form

$$L_{i1}(u_1) + L_{i2}(v_1) + L_{i3}(w_1) = 0, \quad i = 1, 2, 3, \quad (17a)$$

$$B_{i1}(u_1) + B_{i2}(v_1) + B_{i3}(w_1) = 0, \quad i = 1, 2, 3, \quad (17b)$$

where L_{ij} and B_{ij} are differential operators of second order.

Solution Methodology

In solving problems using the Galerkin technique, three methods can be used to choose trial functions: the interior method, the boundary method, and the mixed method. In this study, the mixed method (Mikhlin, 1964, Bolotin, 1963, Finlayson, 1972) is employed to overcome the complexity of finding trial functions that satisfy either the differential Eqs. (17a) or the boundary conditions (17b). Use of the Galerkin procedure requires that the interior and boundary weighted residuals vanish. For the first differential equation and boundary condition corresponding to $i = 1$ in (17), these appear as

$$\int_V \hat{u}_j[L_{11}(u_1) + L_{12}(v_1) + L_{13}(w_1)]dV = 0, \quad (18a)$$

$$\int_S \hat{u}_j[B_{11}(u_1) + B_{12}(v_1) + B_{13}(w_1)]dS = 0, \quad (18b)$$

where $\hat{u}_j$ is the jth term of the trial functions of the displacement u_1. Similarly, those residuals can be written for the second and third equations corresponding to $i = 2, 3$ in (17) by subsequently replacing $\hat{u}_j$ with $\hat{v}_j$ and $\hat{w}_j$, respectively. After per-

forming integration by parts with respect to r on (18a) and combining it with (18b), and doing similar procedures for the other two sets of equations, we can obtain the following three sets of governing equations:

$$\int_V \{\hat{u}_j[L'_{11}(u_1) + L'_{12}(v_1) + L'_{13}(w_1)] - \hat{u}_{j,r}[B'_{11}(u_1) + B'_{12}(v_1) + B'_{13}(w_1)]\}dV = 0, \quad (19a)$$

$$\int_V \{\hat{v}_j[L'_{21}(u_1) + L'_{22}(v_1) + L'_{23}(w_1)] - \hat{v}_{j,r}[B'_{21}(u_1) + B'_{22}(v_1) + B'_{23}(w_1)]\}dV = 0, \quad (19b)$$

$$\int_V \{\hat{w}_j[L'_{31}(u_1) + L'_{32}(v_1) + L'_{33}(w_1)] - \hat{w}_{j,r}[B'_{31}(u_1) + B'_{32}(v_1) + B'_{33}(w_1)]\}dV = 0, \quad (19c)$$

where the modified operators L'_{ij} and B'_{ij} are given in Appendix A.

Considering the fixed boundary conditions at the longitudinal edges $z = 0, L$, trial functions for the displacements are chosen as

$$u_1 = \sum_{k=1}^{K_1}\sum_{m=1}^{M_1} P_k(r)[A_{kmn}\,\mathrm{Sin}\,(n\theta) + B_{kmn}\,\mathrm{Cos}\,(n\theta)]\,\mathrm{Sin}\,(\lambda_m z), \quad (20a)$$

$$v_1 = \sum_{k=1}^{K_2}\sum_{m=1}^{M_2} P_k(r)[C_{kmn}\,\mathrm{Sin}\,(n\theta) + D_{kmn}\,\mathrm{Cos}\,(n\theta)]\,\mathrm{Sin}\,(\lambda_m z), \quad (20b)$$

$$w_1 = \sum_{k=0}^{K_3-1}\sum_{m=1}^{M_3} P_k(r)[E_{kmn}\,\mathrm{Sin}\,(n\theta) + F_{kmn}\,\mathrm{Cos}\,(n\theta)]\,\mathrm{Sin}\,(\lambda_m z), \quad (20c)$$

where $P_k(r)$ is a kth term set of Legendre polynomials, $\lambda_m = m\pi/L$, and A_{kmn}, B_{kmn}, C_{kmn}, D_{kmn}, E_{kmn}, F_{kmn} are unknown coefficients. The integer values n and m in Eqs. (20) represent the number of waves around the circumference and along the length of the cylinder, respectively. Upon substituting Eqs. (20) into Eqs. (19) and integrating, we obtain six sets of linear algebraic equations. The $(q + k)$th terms for the first and second sets of the $(K_1 \times M_1)$ equations are, respectively,

$$\sum_{k=1}^{K_1}\sum_{m=1}^{M_1}[(\Gamma^{(11)}_{qk} + \lambda_m^2\Gamma^{(14)}_{qk} + \Psi^{(11)}_{qk})\Phi^{(1)}_{pm}A_{kmn} - \bar{M}(\Lambda^{(11)}_{qk})\lambda_m\Phi^{(2)}_{pm}B_{kmn}] - \sum_{k=1}^{K_2}\sum_{m=1}^{M_2}[(\Gamma^{(12)}_{qk} + \Psi^{(12)}_{qk})\Phi^{(1)}_{pm}D_{kmn} - \bar{M}(\Lambda^{(12)}_{qk})\lambda_m\Phi^{(2)}_{pm}C_{kmn}] + \sum_{k=0}^{K_3-1}\sum_{m=1}^{M_3}[(\Gamma^{(13)}_{qk} + \Psi^{(13)}_{qk})\lambda_m\Phi^{(2)}_{pm}E_{kmn} - \bar{M}(\Lambda^{(13)}_{qk})\Phi^{(1)}_{pm}F_{kmn}] = 0, \quad (21a)$$

$$\sum_{k=1}^{K_1}\sum_{m=1}^{M_1}[(\Gamma^{(11)}_{qk} + \lambda_m^2\Gamma^{(14)}_{qk} + \Psi^{(11)}_{qk})\Phi^{(1)}_{pm}B_{kmn} + \bar{M}(\Lambda^{(11)}_{qk})\lambda_m\Phi^{(2)}_{pm}A_{kmn}] + \sum_{k=1}^{K_2}\sum_{m=1}^{M_2}[(\Gamma^{(12)}_{qk} + \Psi^{(12)}_{qk})\Phi^{(1)}_{pm}C_{kmn} + \bar{M}(\Lambda^{(12)}_{qk})\lambda_m\Phi^{(2)}_{pm}D_{kmn}] + \sum_{k=0}^{K_3-1}\sum_{m=1}^{M_3}[(\Gamma^{(13)}_{qk} + \Psi^{(13)}_{qk})\lambda_m\Phi^{(2)}_{pm}F_{kmn} + \bar{M}(\Lambda^{(13)}_{qk})\Phi^{(1)}_{pm}E_{kmn}] = 0, \quad (21b)$$

the $(q + k)$th terms for the third and fourth sets of the $(K_2 \times M_2)$ equations are, respectively,

$$-\sum_{k=1}^{K_1}\sum_{m=1}^{M_1}[(\Gamma^{(21)}_{qk} + \Psi^{(21)}_{qk})\Phi^{(1)}_{pm}B_{kmn} - \bar{M}(\Lambda^{(21)}_{qk})\lambda_m\Phi^{(2)}_{pm}A_{kmn}] + \sum_{k=1}^{K_2}\sum_{m=1}^{M_2}[(\Gamma^{(22)}_{qk} + \lambda_m^2\Gamma^{(24)}_{qk} + \Psi^{(22)}_{qk})\Phi^{(1)}_{pm}C_{kmn} - \bar{M}(\Lambda^{(22)}_{qk})\lambda_m\Phi^{(2)}_{pm}D_{kmn}] - \sum_{k=0}^{K_3-1}\sum_{m=1}^{M_3}[(\Gamma^{(23)}_{qk} + \Psi^{(23)}_{qk})\lambda_m\Phi^{(2)}_{pm}F_{kmn} - \bar{M}(\Lambda^{(23)}_{qk})\Phi^{(1)}_{pm}E_{kmn}] = 0, \quad (21c)$$

$$\sum_{k=1}^{K_1}\sum_{m=1}^{M_1}[(\Gamma^{(21)}_{qk} + \Psi^{(21)}_{qk})\Phi^{(1)}_{pm}A_{kmn} + \bar{M}(\Lambda^{(21)}_{qk})\lambda_m\Phi^{(2)}_{pm}B_{kmn}] + \sum_{k=1}^{K_2}\sum_{m=1}^{M_2}[(\Gamma^{(22)}_{qk} + \lambda_m^2\Gamma^{(24)}_{qk} + \Psi^{(22)}_{qk})\Phi^{(1)}_{pm}D_{kmn} + \bar{M}(\Lambda^{(22)}_{qk})\lambda_m\Phi^{(2)}_{pm}C_{kmn}] + \sum_{k=0}^{K_3-1}\sum_{m=1}^{M_3}[(\Gamma^{(23)}_{qk} + \Psi^{(23)}_{qk})\lambda_m\Phi^{(2)}_{pm}E_{kmn} + \bar{M}(\Lambda^{(23)}_{qk})\Phi^{(1)}_{pm}F_{kmn}] = 0, \quad (21d)$$

and finally, the $(q + k)$th terms for the fifth and sixth sets of the $(K_3 \times M_3)$ equations are, respectively,

$$\sum_{k=1}^{K_1}\sum_{m=1}^{M_1}[(\Gamma^{(31)}_{qk} + \Psi^{(31)}_{qk})\lambda_m\Phi^{(2)}_{pm}A_{kmn}] - \sum_{k=1}^{K_2}\sum_{m=1}^{M_2}[(\Gamma^{(32)}_{qk} + \Psi^{(32)}_{qk})\lambda_m\Phi^{(2)}_{pm}D_{kmn} - \bar{M}(\lambda_m^2\Lambda^{(32)}_{qk})\Phi^{(1)}_{pm}C_{kmn}] + \sum_{k=0}^{K_3-1}\sum_{m=1}^{M_3}[(\Gamma^{(33)}_{qk} + \lambda_m^2\Gamma^{(34)}_{qk} + \Psi^{(33)}_{qk})\Phi^{(1)}_{pm}E_{kmn} - \bar{M}(\Lambda^{(33)}_{qk})\lambda_m\Phi^{(2)}_{pm}F_{kmn}] = 0, \quad (21e)$$

$$\sum_{k=1}^{K_1}\sum_{m=1}^{M_1}[(\Gamma^{(31)}_{qk} + \Psi^{(31)}_{qk})\lambda_m\Phi^{(2)}_{pm}B_{kmn}] + \sum_{k=1}^{K_2}\sum_{m=1}^{M_2}[(\Gamma^{(32)}_{qk} + \Psi^{(32)}_{qk})\lambda_m\Phi^{(2)}_{pm}C_{kmn} + \bar{M}(\lambda_m^2\Lambda^{(32)}_{qk})\Phi^{(1)}_{pm}D_{kmn}] + \sum_{k=0}^{K_3-1}\sum_{m=1}^{M_3}[(\Gamma^{(33)}_{qk} + \lambda_m^2\Gamma^{(34)}_{qk} + \Psi^{(33)}_{qk})\Phi^{(1)}_{pm}F_{kmn} + \bar{M}(\Lambda^{(33)}_{qk})\lambda_m\Phi^{(2)}_{pm}E_{kmn}] = 0. \quad (21f)$$

In Eqs. (21) above, constants from integration of the trigonometric functions in the z direction are denoted by

$$\Phi^{(1)}_{pm} = \int_0^L \mathrm{Sin}\,(\lambda_p z)\,\mathrm{Sin}\,(\lambda_m z)dz, \quad (22a)$$

$$\Phi^{(2)}_{pm} = \int_0^L \mathrm{Sin}\,(\lambda_p z)\,\mathrm{Cos}\,(\lambda_m z)dz, \quad (22b)$$

and those from integration with respect to r are

$$\Gamma^{(ij)}_{qk} = \int_{R_1}^{R_2} P_q D^S_{ij}(P_k)rdr, \quad (23a)$$

$$\Lambda^{(ij)}_{qk} = \int_{R_1}^{R_2} P_q D^G_{ij}(P_k)rdr, \quad (23b)$$

$$\Psi^{(ij)}_{qk} = -\int_{R_1}^{R_2} P_{q,r}K_{ij}(P_k)rdr, \quad (23c)$$

where D^S_{ij} and D^G_{ij} are the ensuing r-dependent terms after substituting the trial displacement functions in (20) into the operators L'_{ij} in (19). Similarly K_{ij} are the ensuing r-dependent terms after substituting (20) into B'_{ij} in (19). D^S_{ij}, D^G_{ij}, and K_{ij} are given explicitly in Appendix B.

Equations (21) yield $2 \times (K_1 \times M_1 + K_2 \times M_2 + K_3 \times M_3)$ algebraic equations. However, it can be noted that the terms

Table 1 Aspect ratios of an isotropic cylinder corresponding to the results of Figs. 2 and 3

	L/R_c, R_c/h							
	n							
Z	2	3	4	5	6	7	8	9
10000	21.05, 23.66	14.03, 53.24	10.52, 94.64	8.419, 147.9	7.016, 212.9	6.014, 289.8	5.262, 378.6	4.677, 479.1
5000	17.28, 17.56	11.52, 39.50	8.639, 70.22	6.912, 109.7	5.760, 158.0	4.937, 215.1	4.320, 280.9	3.840, 355.5
2000	13.31, 11.84	8.870, 26.65	6.652, 47.38	5.322, 74.03	4.435, 106.6	3.801, 145.1	3.326, 189.5	2.957, 239.8
1000	10.79, 9.002	7.194, 20.25	5.396, 36.01	4.317, 56.26	3.597, 81.02	3.083, 110.3	2.698, 144.0	2.398, 182.3
500	8.671, 6.972	5.781, 15.69	4.335, 27.89	3.468, 43.57	2.890, 62.74	2.477, 85.40	2.168, 111.5	1.927, 141.2
200	6.362, 5.180	4.241, 11.66	3.181, 20.72	2.545, 32.38	2.121, 46.62	1.818, 63.46	1.590, 82.89	1.414, 104.9
100	4.948, 4.282	3.299, 9.634	2.474, 17.13	1.979, 26.76	1.649, 38.54	1.414, 52.45	1.237, 68.51	1.100, 86.71
50	3.817, 3.597	2.545, 8.094	1.909, 14.39	1.527, 22.48	1.272, 32.38	1.091, 44.07	0.954, 57.56	0.848, 72.85
20	2.733, 2.807	1.822, 6.315	1.367, 11.23	1.093, 17.54	0.911, 25.26	0.781, 34.38	0.683, 44.91	0.607, 56.83
10	2.246, 2.078	1.497, 4.675	1.123, 8.311	0.898, 12.99	0.749, 18.70	0.642, 25.45	0.562, 33.24	0.499, 42.07

including $\bar{M}$ in (21) have either A_{kmn}, D_{kmn}, E_{kmn} only or B_{kmn}, C_{kmn}, F_{kmn} only. Therefore, Eqs. (21) can be divided into two parts to reduce the dimensions of matrices to be handled. These two partitioned sets of equations are in the form

$$[P]\{\alpha\} + \bar{M}[Q]\{\beta\} = \{0\}, \tag{24a}$$

$$[S]\{\beta\} + \bar{M}[R]\{\alpha\} = \{0\}, \tag{24b}$$

where $\{\alpha\} = \lfloor A_{kmn}, D_{kmn}, E_{kmn} \rfloor^T$ and $\{\beta\} = \lfloor B_{kmn}, C_{kmn}, F_{kmn} \rfloor^T$. The matrices P, Q, R, and S have the dimension of $(K_1 \times M_1) + (K_2 \times M_2) + (K_3 \times M_3)$, respectively. From (24$a$) we obtain

$$\{\alpha\} = -\bar{M}[P]^{-1}[Q]\{\beta\}. \tag{25}$$

Substitution into (24b) yields

$$([S] - \bar{M}^2[G])\{\beta\} = \{0\}, \tag{26}$$

where $[G] = [R][P]^{-1}[Q]$.

Equation (26) constitutes a generalized eigensystem with $\bar{M}^2$ being the eigenvalue. The system has a nontrivial solution if and only if the determinant of $[S] - \bar{M}^2[G]$ vanishes.

Numerical Results and Discussion

Numerical results based on the preceding formulations have been generated for a wide range of geometrical and material parameters affecting the behavior of cylindrical shells under torsional loads. For all cases considered, the critical torsional load was computed using a QR algorithm combined with similarity reduction of general matrix to upper Hessenberg form (Wilkinson and Reinsch, 1971). When calculating eigenvalues, extended precision (28 significant figures) was used. By increasing the integer value of circumferential wave number, n, the lowest eigenvalue corresponding to the critical load was found.

Comparison With Existing Isotropic Shell Solutions. For an isotropic cylinder subjected to torsion, Yamaki (1984) presented numerical results pertaining to the critical shear stress, τ_{cr}, and the corresponding circumferential wave number parameter, $\beta = nL/\pi R_c$, where R_c and L are the radius of the midline surface and the length of the shell, respectively. He employed a direct integration method combined with an iterative technique to Donnell's buckling equations and concluded that Donnell's equations yielded sufficiently accurate results when n is greater than 4. The inaccuracy of the Donnell's equations for the cases with low values of n refers to the shallow shell approximation that omits the in-plane displacement component in certain kinematic relations. It should be noted that he specified the geometric property of the shell by only one parameter $Z = \sqrt{1 - \nu^2}(L/R_c)^2(R_c/h)$, which is known as the Batdorf parameter, where h is the thickness of the shell, and then minimized eigenvalues with respect to the wave number by treating β as a continuous variable.

In order to compare Yamaki's results with those from this study, a combination of the geometric parameters with an assumed integer value of n for a particular isotropic cylinder was selected so as to correspond to the published values of Z and β by Yamaki. For convenience, these parameters (L/R_c and R_c/h) are given in Table 1. A range of n from 2 to 9 was used and R_c was set to 0.1905 m.

In addition to the shell theory results by Yamaki, those from a simplified formula derived by Donnell (1933) were also compared with the present elasticity solutions. Donnell presented the following formula for the critical shear stress of ends-fixed short and moderately long shells subjected to torsion:

$$\tau_{cr} = \frac{E}{(1 - \nu^2)} \frac{h^2}{L^2} \left[4.6 + \sqrt{7.8 + 1.67 \left(\sqrt{1 - \nu^2} \frac{L^2}{2hR_c} \right)^{3/2}} \right]. \tag{27}$$

The critical torsional load, M_{cr}, can then be calculated:

$$M_{cr} = \tau_{cr} \frac{2\pi}{3} (R_2^3 - R_1^3). \tag{28}$$

Table 2 shows critical torsional loads, as predicted by the present three-dimensional elasticity formulation, compared with those predicted by Donnell's formula and Yamaki for a typical value of circumferential wave number $n = 5$. Since an isotropic cylinder was investigated, Young's modulus E was assumed to

Table 2 Comparison of results for an isotropic cylinder (n = 5)

	Critical torsional loads ($N \cdot m \times 10^{-7}$)		
Z	Elasticity	Donnell (% increase vs. Elasticity)	Yamaki (% increase vs. Elasticity)
10000	1.565	1.610 (2.82%)	1.578 (0.82%)
5000	3.366	3.491 (3.70%)	3.393 (0.79%)
2000	9.238	9.740 (5.44%)	9.312 (0.81%)
1000	18.95	20.32 (7.26%)	19.10 (0.79%)
500	37.58	41.20 (9.64%)	37.86 (0.74%)
200	86.97	98.96 (13.8%)	87.54 (0.65%)
100	157.2	184.8 (17.5%)	158.1 (0.57%)
50	287.0	348.0 (21.3%)	289.3 (0.80%)
20	737.3	916.7 (24.3%)	759.1 (2.95%)
10	2069	2633 (27.3%)	2271 (9.76%)

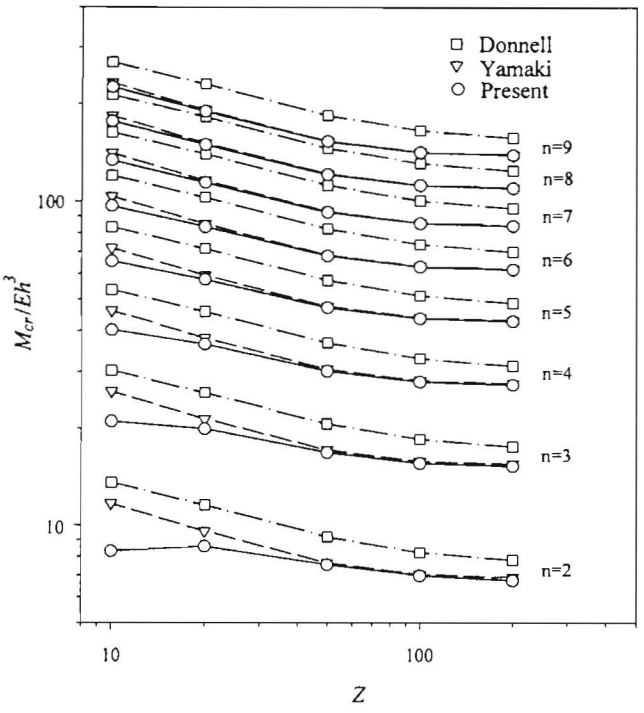

Fig. 2 Comparison of critical loads for an isotropic cylinder ($Z \leq 200$)

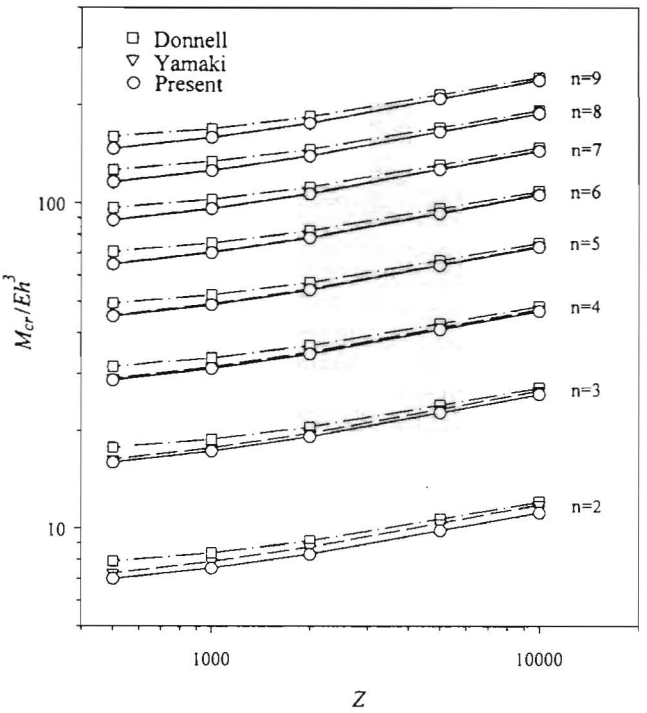

Fig. 3 Comparison of critical loads for an isotropic cylinder ($Z \geq 500$)

be unity for convenience and Poisson's ratio ν was taken as 0.3.

It is clearly seen from Table 2 that Yamaki's results are much closer to the elasticity solutions than those from the Donnell's simplified formula and that both shell theory solutions result in nonconservative critical torsional loads. Discrepancies between the elasticity solution and Donnell's formula increase as the parameter Z becomes small, as is the case for short and thick cylinders. On the other hand, differences between the Yamaki's result and elasticity solution are independent of values of Z as long as Z is greater than 50. Discrepancies increase drastically for very short and moderately thick cylinders with values of Z less than 20.

Critical torsional loads for the same isotropic cylinder that buckles into wave numbers other than 5 were also calculated and compared with those from shell theories. Results are shown graphically in Figs. 2 and 3, where the nondimensionalized critical torque M_{cr}/Eh^3 is plotted against the parameter Z. Similar observations can be made for the cases with n other than 5. In addition, the larger the wave number n for the same values of Z, the smaller the differences between both shell theory approaches and the elasticity solutions. It should be noted that circumferential wave numbers used to set the input parameters for given values of Z, are proven to correspond to the lowest eigenvalues from the elasticity solutions for all cases studied.

To examine the convergence of the present eigenvalue solution as sufficient numbers of displacement functions are retained, values for critical torsional loads for the previously discussed isotropic cylindrical shell ($Z = 10$, $L/R_c = 0.898$, $R_c/h = 12.99$, $n = 5$) were generated as the numbers of terms in r and z increase by one, respectively. The number of terms in r and in z describe numbers of the upper indices, K_i and M_i, respectively, in Eq. (20), where $i = 1, 2, 3$. Equal numbers for K_i (i.e., $K_1 = K_2 = K_3$) and M_i (i.e., $M_1 = M_2 = M_3$) were used for the displacements u_1, v_1, w_1.

Results are given in Table 3, which clearly shows that the critical torsional load is monotonically converging from above as the number of terms in r and z increases. An acceptable converged value for the critical load occurs when addition of one term in z as well as in r yields a difference between subsequent values less than 0.01 percent. Therefore, for this case the converged critical load is obtained by employing five terms in r and 21 terms in z, or 5×21 terms.

Same monotonic convergence is detected for all other studied isotropic cylinder cases, but convergence tables are not presented here because of limited space. Instead, solution sizes, which provide converged values of the critical torsional loads,

Table 3 Convergence of critical loads for an isotropic cylinder ($Z = 10$, $n = 5$)

	Critical torsional loads ($N \cdot m \times 10^{-7}$)		
No. of terms in z	No. of terms in r		
	3	4	5
1	6693.7	6667.5	6667.4
2	2243.0	2208.4	2208.0
3	2167.8	2132.6	2132.3
4	2141.5	2105.7	2105.3
5	2129.3	2093.0	2092.6
6	2122.6	2085.9	2085.4
7	2118.5	2081.5	2081.0
8	2115.7	2078.6	2078.1
9	2113.9	2076.6	2076.0
10	2112.5	2075.1	2074.5
11	2111.4	2073.9	2073.4
12	2110.6	2073.1	2072.5
13	2110.0	2072.4	2071.7
14	2109.5	2071.8	2071.2
15	2109.1	2071.4	2070.7
16	2108.7	2071.0	2070.3
17	2108.4	2070.7	2070.0
18	2108.2	2070.5	2069.7
19	2108.0	2070.3	2069.5
20	2107.8	2070.1	2069.2
21	2107.6	2069.9	2069.1

Table 4 Number of terms required for convergence of critical loads for an isotropic cylinder

	(No. of terms in r) x (No. of terms in z)							
	n							
Z	2	3	4	5	6	7	8	9
10000	4x30	3x31	3x34	3x34	3x35	3x35	3x36	3x36
5000	4x29	4x31	3x33	3x33	3x34	3x35	3x35	3x36
2000	4x27	4x28	4x31	4x31	3x32	3x33	3x34	3x34
1000	4x25	4x26	4x30	4x30	4x31	3x32	3x33	3x33
500	4x24	4x24	4x27	4x27	4x29	4x30	4x31	4x32
200	4x20	4x22	4x25	4x25	4x26	4x28	4x29	4x30
100	5x19	4x20	4x24	4x24	4x25	4x26	4x27	4x28
50	5x17	4x19	4x23	4x23	4x24	4x25	4x26	4x28
20	5x15	5x18	4x22	4x22	4x23	4x25	4x26	4x27
10	5x13	5x16	5x21	5x21	4x22	4x23	4x24	4x25

are summarized in Table 4. When n is larger than 5, the use of Legendre polynomials containing up to four terms provides accepted convergence values. Maximum number of terms in r for all cases considered here is 5. It is clearly seen from Table 4 that a larger number of z terms is required for a longer cylinder with a larger value of Z regardless of the circumferential wave number. However, for a given value of Z the rate of convergence is slightly slower as the wave number n increases even though a higher value of n refers to a shorter cylinder.

Comparison With Existing Orthotropic Shell Solutions. Before discussing accuracy of the shell theory results for orthotropic cylinders, it is now appropriate to quote a study performed by Etitum and Dong (1995). They calculated torsional buckling loads of cross-ply and angle-ply cylinders by using a three-dimensional semi-analytical finite element method, based on Biot's incremental deformation theory (Biot, 1965) and then compared the results with those obtained from the classical and the first-order shear deformation formulations based on the Flügge shell theory. They concluded that for thin geometry ($R_c/h = 100$), classical theory can be trusted to give accurate results over a reasonably wide range of normalized wavelength ratio L/R_c. They also showed that shell theories and three-dimensional formulation do not correlate well at all for a relatively thick cylinder ($R_c/h = 10$). In this case, shell theory results can be lower or higher than those obtained from three-dimensional theory depending upon the values of L/R_c.

In the literature, there is a limited number of shell theory based articles dealing with torsion of orthotropic cylinders having fixed ends (Simitses, 1967, 1968; Tabiei and Simitses, 1994). Tabiei and Simitses (1994) performed an extensive parametric study of laminated cylindrical shells under torsion by employing Donnell-type kinematic relations when deriving the equilibrium equations and then employing Sanders-type relations in the buckling equations. They compared numerical results from classical shell theory (CL), first-order shear deformation theory (FOSD), and higher-order shear deformation theory (HOSD).

Table 5 shows critical torsional loads of graphite/epoxy cylinders predicted by the present three-dimensional elasticity formulation along with those from Tabiei and Simitses (1994) based on the various shell theories. The material properties of the Graphite/Epoxy cylinder considered herein are

$$E_{11} = E_{22} = 9.928 \times 10^9 \text{ N/m}^2,$$

$$E_{33} = 149.617 \times 10^9 \text{ N/m}^2,$$

$$G_{12} = 2.551 \times 10^9 \text{ N/m}^2, \quad G_{13} = G_{23} = 4.481 \times 10^9 \text{ N/m}^2,$$

$$\nu_{12} = 0.45, \quad \nu_{13} = \nu_{23} = 0.0186.$$

Radius of the centerline of the cylinder, R_c is set to 0.1905 m and the length is varied such that $L/R_c = 1, 2, 5$. The thickness of the cylinder is also varied to correspond to R_c/h ratios equal to 100, 60, 30, and 15. On the third column of Table 5, Batdorf parameter $\tilde{z}$ for orthotropic cylinder, corresponding to the shell geometric parameter Z is indicated. It should be noted that $\tilde{z}$ depends not only on the geometry but also on the stiffness constants (Nemeth, 1994), and is defined as

$$\tilde{z} = \frac{L^2(Q_{11}Q_{22} - Q_{12}^2)^{1/2}}{R_c\sqrt{12}(Q_{11}Q_{22}D_{11}D_{22})^{1/4}}, \tag{29}$$

where stiffness constants Q_{ij} and flexural rigidity D_{ij} of a cylindrical shell are (1 ≡ axial, 2 ≡ circumferential),

$$Q_{11} = \frac{hE_{11}}{1 - \nu_{12}\nu_{21}}; \quad Q_{22} = \frac{hE_{22}}{1 - \nu_{12}\nu_{21}};$$

$$Q_{12} = \frac{h\nu_{12}E_{22}}{1 - \nu_{12}\nu_{21}}; \quad D_{ij} = \frac{h^2}{12}Q_{ij}. \tag{30}$$

The data in Table 5 are also shown graphically in Fig. 4 by normalizing the critical torsional load to $M_{cr}/E_{22}h^3$. It is clearly seen from Table 5 and Fig. 4 that results from shell theories are reasonably close to the elasticity solutions as long as the cylinder is long or thin. More specifically, when the ratio L/R_c is set at 5, the data from all approaches agree remarkably well over the entire range of the R_c/h ratios considered. Furthermore, all shell theories predict slightly lower values for the critical loads. However, for the case of short cylinder ($L/R_c = 1$) classical shell theory predicts much higher values when the cylinder is moderately thick ($R_c/h \leq 30$), while shear deformation theories provide reasonable values for the critical torsional loads. When L/R_c is 2, the classical theory results are higher than the elasticity solutions except for the case of $R_c/h = 60$, but shear deformation theory results are lower except $R_c/h = 100$ case.

Higher-order shear deformation theory gave conservative values for all cases except for the case of $L/R_c = 2$, $R_c/h = 100$.

Table 5 Comparison of results for an orthotropic cylinder

	Critical torsional loads ($N \cdot m \times 10^4$) / Wave number						
Geometry			Elasticity	CL*	FOSD*	HOSD*
L/R_c	R_c/h	$\tilde{z}$		(% increase vs. Elasticity)	(% increase vs. Elasticity)	(% increase vs. Elasticity)
5	100	2493	.8418/7	.8277 / 7 (-1.67%)	.8277 / 7 (-1.67%)	.8277 / 7 (-1.67%)
5	60	1496	2.552/6	2.515 / 6 (-1.44%)	2.515 / 6 (-1.44%)	2.515 / 6 (-1.44%)
5	30	748.1	12.00/5	11.78 / 5 (-1.84%)	11.74 / 5 (-2.18%)	11.72 / 5 (-2.33%)
5	15	374.0	58.56/4	58.33 / 4 (-0.38%)	56.33 / 4 (-3.80%)	56.01 / 4 (-4.34%)
2	100	399.0	1.255/9	1.297 / 10 (3.42%)	1.293 / 10 (3.06%)	1.293 / 10 (3.06%)
2	60	239.4	4.217/7	4.193 / 7 (-0.55%)	4.173 / 7 (-1.04%)	4.155 / 7 (-1.47%)
2	30	119.7	23.57/6	23.96 / 6 (1.67%)	23.32 / 6 (-1.05%)	23.01 / 6 (-2.40%)
2	15	59.84	138.9/5	158.2 / 5 (13.9%)	134.6 / 5 (-3.07%)	130.0 / 5 (-6.41%)
1	100	99.74	2.429/11	2.456 / 11 (1.09%)	2.435 / 11 (0.25%)	2.396 / 11 (-1.35%)
1	60	59.84	9.605/10	9.985 / 10 (3.96%)	9.666 / 10 (0.64%)	9.504 / 10 (-1.05%)
1	30	29.92	62.32/9	73.47 / 8 (17.9%)	61.91 / 9 (-0.66%)	59.51 / 9 (-4.50%)
1	15	14.96	347.6/8	575.0 / 7 (65.4%)	329.6 / 8 (-5.17%)	309.2 / 8 (-11.0%)

* Tabiei and Simitses (1994)

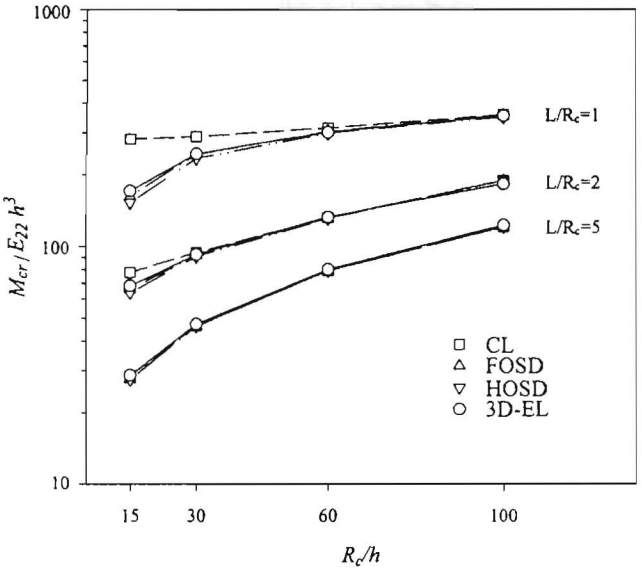

Fig. 4 Comparison of critical loads for an orthotropic cylinder

The results from classical theory and first-order shear deformation theory are higher or lower, depending on L/R_c and R_c/h. It should be mentioned on the basis of the results compared herein that there is no trend on the conservatism of the critical loads from shell theories as in the isotropic cases.

Figure 5 shows a comparison of normalized critical torsional loads with respect to the Batdorf parameter $\tilde{z}$. Even though the data from shell theories compared herein are limited, it can be noted that for the value of $\tilde{z}$ above about 100, shell theories are adequate to predict critical torsional load of an orthotropic cylinder.

The circumferential wave number n that a cylinder buckles into is also shown in Table 5. Integer wave numbers calculated from the shell theories and elasticity formulation agreed in most cases. However, all shell theories predicted different wave numbers for the case of $L/R_c = 2$, $R_c/h = 100$, and so did the classical shell theory for the cases of $L/R_c = 1$, $R_c/h = 15$ and $L/R_c = 1$, $R_c/h = 30$.

It should be noted that the critical load is also monotonically converging for all cases of orthotropic construction considered herein, as it is for an isotropic cylinder. Four terms in r are employed to provide convergence within 0.01 percent for all cases except the shortest and thickest cylinder with $L/R_c = 1$, $R_c/h = 15$, which needs five terms. Maximum number of z terms needed is 25 when $L/R_c = 1$, $R_c/h = 15$. For a given L/R_c ratio, the number of terms in z needed decreases as the ratio R_c/h becomes small.

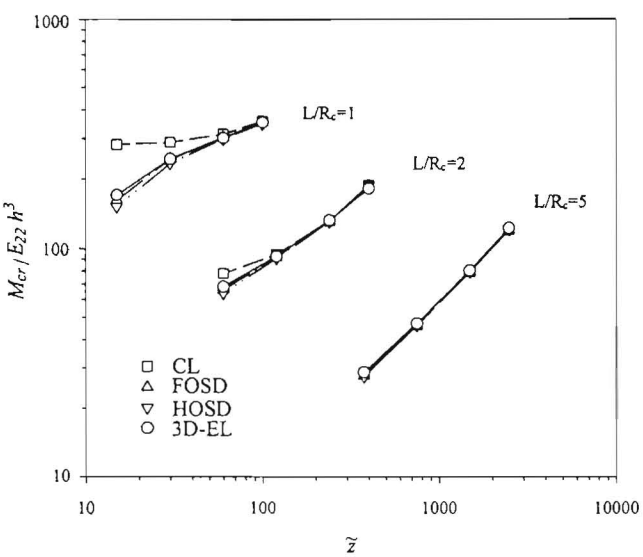

Fig. 5 Variation of critical loads for an orthotropic cylinder with respect to $\tilde{z}$

Table 6 Critical torsional loads of an isotropic cylinder

	Critical torsional loads ($N \cdot m \times 10^6$) / Wave number				
	R_2/R_1				
L/R_2	1.01	1.05	1.1	1.15	1.2
1	2.262/10	101.6/6	516.7/5	1238/4	2164/4
2	1.513/8	54.84/5	247.0/4	565.2/3	987.5/3
3	1.232/7	41.70/4	182.3/3	404.3/3	725.9/3
4	1.070/6	35.81/4	148.9/3	344.7/3	633.1/3
5	.9650/6	32.99/4	132.4/3	316.5/3	527.4/2
6	.8784/5	29.25/3	123.2/3	288.9/2	451.4/2
7	.8111/5	26.47/3	117.5/3	250.4/2	403.2/2
8	.7687/5	24.68/3	113.9/3	224.7/2	371.2/2
9	.7304/4	23.46/3	102.9/2	207.0/2	349.0/2
10	.6816/4	22.60/3	93.61/2	194.4/2	333.2/2

Parametric Study. Having established confidence in the methodology and assessed the accuracy of shell theory results, an extensive parametric study is performed to provide accurate values for the critical torsional loads of isotropic and orthotropic cylindrical shells. Results presented herein can be used as references for future studies employing shell theory.

For the isotropic cylinder Young's modulus $E = 14$ GN/m^2 and Poisson's ratio $\nu = 0.3$ are assumed. Orthotropic materials considered here are typical glass/epoxy and graphite/epoxy with circumferential reinforcements, having the following properties:

$$\text{glass/epoxy: } E_{11} = E_{33} = 14.0 \times 10^9 \text{ N/m}^2,$$

$$E_{22} = 57.0 \times 10^9 \text{ N/m}^2,$$

$$G_{12} = G_{23} = 5.7 \times 10^9 \text{ N/m}^2, \; G_{13} = 5.0 \times 10^9 \text{ N/m}^2,$$

$$\nu_{12} = 0.068, \; \nu_{13} = 0.400, \; \nu_{23} = 0.277,$$

$$\text{graphite/epoxy: } E_{11} = 9.9 \times 10^9 \text{ N/m}^2,$$

$$E_{22} = 140.0 \times 10^9 \text{ N/m}^2,$$

$$E_{33} = 9.1 \times 10^9 \text{ N/m}^2, \quad G_{12} = 4.7 \times 10^9 \text{ N/m}^2,$$

$$G_{13} = 5.9 \times 10^9 \text{ N/m}^2, \quad G_{12} = 4.3 \times 10^9 \text{ N/m}^2$$

$$\nu_{12} = 0.020, \; \nu_{13} = 0.533, \; \nu_{23} = 0.300,$$

where the subscripts 1, 2, 3 correspond to r, θ, and z-directions, respectively.

The outer cylinder radius R_2 is set to 1 m and the ratio L/R_2 is varied from 1 to 10. A range of outer versus inner radii R_2/R_1 from thin (1.01) to thick (1.20) is examined.

Tables 6 through 8 show critical torsional loads and wave numbers around the circumference for the isotropic, the glass/epoxy, and the graphite/epoxy cylinders. In general, critical torsional loads of the graphite/epoxy cylinder are higher than those of the glass/epoxy cylinder because of the stronger reinforcements. As the cylinder becomes thicker or longer, it buckles into a lower circumferential wave number n. For given shell geometries, the buckling wave number of the isotropic cylinder is the highest followed by the glass/epoxy cylinder and then the graphite/epoxy cylinder.

Table 7 Critical torsional loads of a glass/epoxy cylinder

Critical torsional loads ($N \cdot m \times 10^6$) / Wave number

	R_2/R_1				
L/R_2	1.01	1.05	1.1	1.15	1.2
1	3.811/9	141.7/5	668.2/4	1560/4	2693/4
2	2.832/7	88.00/4	373.3/3	821.6/3	1434/3
3	2.423/6	74.92/4	294.3/3	672.0/3	1168/2
4	2.181/5	66.12/3	265.7/3	602.2/2	933.6/2
5	1.981/5	59.24/3	252.3/3	510.8/2	816.7/2
6	1.874/5	55.41/3	233.7/2	458.2/2	750.8/2
7	1.722/4	53.07/3	209.1/2	425.6/2	710.1/2
8	1.618/4	51.54/3	192.8/2	404.1/2	683.5/2
9	1.548/4	50.49/3	181.6/2	389.2/2	665.1/2
10	1.499/4	47.91/2	173.5/2	378.5/2	651.9/2

Table 8 Critical torsional loads of a graphite/epoxy cylinder

Critical torsional loads ($N \cdot m \times 10^6$) / Wave number

	R_2/R_1				
L/R_2	1.01	1.05	1.1	1.15	1.2
1	4.716/7	153.5/4	682.1/4	1558/4	2621/3
2	3.753/6	108.4/4	413.2/3	904.0/3	1528/3
3	3.305/5	92.00/3	361.1/3	762.8/3	1175/2
4	3.043/5	83.69/3	338.8/2	643.5/2	1015/2
5	2.767/4	79.71/3	296.2/2	585.4/2	938.7/2
6	2.587/4	77.51/3	272.0/2	553.0/2	897.1/2
7	2.479/4	73.65/2	257.0/2	533.1/2	871.8/2
8	2.367/3	67.39/2	247.1/2	520.1/2	855.4/2
9	2.201/3	63.10/2	240.3/2	511.2/2	844.2/2
10	2.085/3	60.04/2	235.4/2	504.7/2	836.1/2

Conclusion

The accuracy of shell theory solutions has been assessed through a comparison study for both isotropic and orthotropic cylinders. For isotropic cylinders it was found that Donnell's simplified formula and the direct integration techniques by Yamaki always predict nonconservative values for the critical torsional loads. The results from Donnell's formula deviate increasingly from those obtained by the present solution as the cylinder becomes shorter and thicker. On the other hand, deviation of Yamaki's results is independent of cylinder dimensions unless the shell geometry parameter, Z, is smaller than 50. As the circumferential wave numbers corresponding to the critical load increase, both shell theory solutions provide more accurate values.

The shell theory solution for orthotropic cylinders, which has been compared with the present elasticity formulation, is based on Donnell-type kinematic relations and Sanders-type buckling equations by employing classical, first-order shear deformation, and higher-order shear deformation theories. While both shear deformation theories provide results reasonably close to the three-dimensional elasticity solutions, classical theory predicts much higher critical load values for a short and thick cylinder. However, there is no observed trend regarding the conservatism of the results from the shell theories with respect to three-dimensional elasticity solutions on the basis of the data compared. In general, it can be concluded that shell theories are adequate to predict critical torsional loads of an orthotropic cylinder for the value of Batdorf parameter $\bar{z}$ above 100.

Detailed numerical tables and figures have also been presented that show variation of critical torsional loads over a wide range of length ratio L/R_2 and radii ratio R_2/R_1 for isotropic, glass/epoxy, and graphite/epoxy cylinders. These solutions can be used to evaluate the performance of various proposed shell theories.

Acknowledgment

The financial support of the Federal Highway Administration (U.S. DOT/FHWA Contract No. 61-93-C-00012), the Office of Naval Research, Ship Structure and Systems, S&T Division (Grant N00014-91-J-1892), and the School of Civil & Environmental Engineering at Georgia Institute of Technology are gratefully acknowledged. The authors would like to thank especially Mr. Eric Munley of the Federal Highway Administration and Dr. Y. D. S. Rajapakse of the Office of Naval Research for their encouragement on this study.

References

Ambartsumian, S. A., 1962, "Contributions to the Theory of Anisotropic Layered Shells," ASME *Applied Mechanics Reviews*, Vol. 15, pp. 245–249.

Babich, I. Y., and Kilin, V. I., 1985, "Stability of a Three-Layer Orthotropic Cylindrical Shell Under Axial Compression," *Soviet Applied Mechanics*, Vol. 21, pp. 566–569.

Bert, C. W., and Francis, P. H., 1974, "Composite Material Mechanics: Structural Mechanics," *AIAA Journal*, Vol. 12, pp. 1173–1186.

Biot, M. A., 1965, *Mechanics of Incremental Deformations*, John Wiley and Sons, New York.

Bolotin, V. V., 1963, *Nonconservative Problems of the Theory of Elastic Stability*, Macmillan, New York.

Ciarlet, P. G., 1988, *Mathematical Elasticity, Vol. 1: Three-dimensional Elasticity*, North Holland, Amsterdam.

Danielson, D. A., and Simmonds, J. G., 1969, "Accurate Buckling Equations for Arbitrary and Cylindrical Elastic Shells," *International Journal of Engineering Science*, Vol. 7, pp. 459–468.

Donnell, L. H., 1933, "Stability of Thin-walled Tubes Under Torsion," NACA Report 479.

Etitum, P. and Dong, S. B., 1995, "A Comparative Study of Stability of Laminated Anisotropic Cylinders Under Axial Compression and Torsion," *International Journal of Solids and Structures*, Vol. 32, pp. 1231–1246.

Finlayson, B. A., 1972, *The Method of Weighted Residuals and Variational Principles*, Academic Press, New York.

Flügge, W., 1973, *Stress in Shells*, Springer-Verlag, Berlin.

Kardomateas, G. A., 1993a, "Buckling of Thick Orthotropic cylindrical Shells Under External Pressure," ASME JOURNAL OF APPLIED MECHANICS, Vol. 60, pp. 195–202.

Kardomateas, G. A., 1993b, "Stability Loss in Thick Transversely Isotropic Cylindrical Shells Under Axial Compression," ASME JOURNAL OF APPLIED MECHANICS, Vol. 60, pp. 506–513.

Kardomateas, G. A., and Chung, C. B., 1994, "Buckling of Thick Orthotropic Cylindrical Shells Under External Pressure Based on Non-planar Equilibrium Modes," *International Journal of Solids and Structures*, Vol. 31, pp. 2195–2210.

Kardomateas, G. A., 1995, "Bifurcation of Equilibrium in Thick Orthotropic Cylindrical Shells Under Axial Compression," ASME JOURNAL OF APPLIED MECHANICS, Vol. 62, pp. 43–52.

Kardomateas, G. A., 1996, "Benchmark Three-dimensional Elasticity Solutions for the Buckling of Thick Orthotropic Cylindrical Shells," *Composites, Part B*, Vol. 27B, pp. 569–580.

Mikhlin, S. G., 1964, *Variational Methods in Mathematical Physics*, Macmillan, New York.

Nemeth, M. P., 1994, "Nondimensional Parameters and Equations for Buckling of Anisotropic Shallow Shells," ASME JOURNAL OF APPLIED MECHANICS, Vol. 61, pp. 664–669.

Sanders, J. L. Jr., 1963, "Nonlinear Theories of Thin Shells," *Quarterly of Applied Mathematics*, Vol. 21, pp. 21–26.

Simitses, G. J., 1967, "Instability of Orthotropic cylindrical Shells Under Combined Torsion and Hydrostatic Pressure," *AIAA Journal*, Vol. 5, pp. 1463–1469.

Simitses, G. J., 1968, "Buckling of Eccentrically Stiffened Cylinders Under Torsion," *AIAA Journal*, Vol. 6, pp. 1856–1860.

Simitses, G. J., 1986, "Buckling and Postbuckling of Imperfect Cylindrical Shells," *Proceedings of the ASME Joint PVP and Computer Engineering Division Conference*, Chicago, IL, ASME PVP-119 and NDE-3, pp. 1–11.

Simitses, G. J., 1996, "Buckling of Moderately Thick Laminated Cylindrical Shells: A Review," *Composites, Part B*, Vol. 27, pp. 581–587.

Soldatos, K. P., and Ye, J., 1994, "Three-dimensional Static, Dynamic, Thermoelastic and Buckling Analysis of Homogeneous and Laminated Composite Cylinders," *Composite Structures*, Vol. 29, pp. 131–143.

Tabiei, A., and Simitses, G. J., 1994, "Buckling of Moderately thick, Laminated Cylindrical Shells Under Torsion," *AIAA Journal*, Vol. 32, pp. 639–647.

Tennyson, R. C., 1974, "Buckling of Laminated Composite Cylinders: A Review," *Composites*, Vol. 1, pp. 17–24.

Timoshenko, S. P., and Gere, J. M., 1961, *Theory of Elastic Stability*, 2nd Ed., McGraw-Hill, New York.

Wilkinson, J. H., and Reinsch, C., 1971, *Linear Algebra*, Springer-Verlag, New York.

Yamaki, N., 1984, *Elastic Stability of Circular Cylindrical Shells*, North-Holland, Amsterdam.

Ye, J., and Soldatos, K. P., 1995, "Three-dimensional Buckling Analysis of Laminated Composite Hollow Cylinders and Cylindrical Panels," *International Journal of Solids and Structures*, Vol. 32, pp. 1949–1962.

APPENDIX A

Operators L'_{ij} and B'_{ij} of Eq. (19) are

$$L'_{11}(u_1) = -c_{12}\frac{u_{1,r}}{r} - c_{22}\frac{u_1}{r^2} + c_{66}\frac{u_{1,\theta\theta}}{r^2} + c_{55}u_{1,zz} + 2\bar{M}u_{1,\theta z}, \quad \text{(A1)}$$

$$L'_{12}(v_1) = c_{66}\frac{v_{1,r\theta}}{r} - (c_{22} + c_{66})\frac{v_{1,\theta}}{r^2} - \bar{M}(rv_{1,rz} + 2v_{1,z}), \quad \text{(A2)}$$

$$L'_{13}(w_1) = c_{55}w_{1,rz} - c_{23}\frac{w_{1,z}}{r} - \bar{M}\left(w_{1,r\theta} - \frac{w_{1,\theta}}{r}\right), \quad \text{(A3)}$$

$$L'_{21}(u_1) = c_{12}\frac{u_{1,r\theta}}{r} + (c_{22} + c_{66})\frac{u_{1,\theta}}{r^2} + \bar{M}u_{1,z}, \quad \text{(A4)}$$

$$L'_{22}(v_1) = c_{66}\frac{v_{1,r}}{r} - c_{66}\frac{v_1}{r^2} + c_{22}\frac{v_{1,\theta\theta}}{r^2} + c_{44}v_{1,zz} + \bar{M}v_{1,\theta z}, \quad \text{(A5)}$$

$$L'_{23}(w_1) = (c_{23} + c_{44})\frac{w_{1,\theta z}}{r} - \bar{M}\left(w_{1,r} + \frac{w_{1,\theta\theta}}{r}\right), \quad \text{(A6)}$$

$$L'_{31}(u_1) = c_{13}u_{1,rz} + c_{23}\frac{u_{1,z}}{r}, \quad \text{(A7)}$$

$$L'_{32}(v_1) = (c_{23} + c_{44})\frac{v_{1,\theta z}}{r} - \bar{M}rv_{1,zz}, \quad \text{(A8)}$$

$$L'_{33}(w_1) = c_{44}\frac{w_{1,\theta\theta}}{r^2} + c_{33}w_{1,zz} + \bar{M}w_{1,\theta z}, \quad \text{(A9)}$$

$$B'_{11}(u_1) = c_{11}u_{1,r} + c_{12}\frac{u_1}{r}, \; B'_{12}(v_1) = c_{12}\frac{v_{1,\theta}}{r}, \; B'_{13}(w_1) = c_{13}w_{1,z}, \quad \text{(A10)}$$

$$B'_{21}(u_1) = c_{66}\frac{u_{1,\theta}}{r}, \; B'_{22}(v_1) = c_{66}v_{1,r} - c_{66}\frac{v_1}{r}, \; B'_{23}(w_1) = 0, \quad \text{(A11)}$$

$$B'_{31}(u_1) = c_{55}u_{1,z}, \; B'_{32}(v_1) = 0, \; B'_{33}(w_1) = c_{55}w_{1,r}. \quad \text{(A12)}$$

APPENDIX B

Operators D^S_{ij} and D^G_{ij} of Eq. (23) are

$$D^S_{11}(P_k) = -\left(\frac{c_{12}}{r}\right)P_{k,r} - \left(\frac{c_{22} + n^2c_{66}}{r^2}\right)P_k, \quad \text{(B1)}$$

$$D^S_{12}(P_k) = \left(\frac{nc_{66}}{r}\right)P_{k,r} - \left(\frac{nc_{22} + nc_{66}}{r^2}\right)P_k, \quad \text{(B2)}$$

$$D^S_{13}(P_k) = (c_{55})P_{k,r} - \left(\frac{c_{23}}{r}\right)P_k, \; D^S_{14}(P_k) = -(c_{55})P_k, \quad \text{(B3)}$$

$$D^S_{21}(P_k) = \left(\frac{nc_{12}}{r}\right)P_{k,r} + \left(\frac{nc_{22} + nc_{66}}{r^2}\right)P_k, \quad \text{(B4)}$$

$$D^S_{22}(P_k) = \left(\frac{c_{66}}{r}\right)P_{k,r} - \left(\frac{n^2c_{22} + c_{66}}{r^2}\right)P_k, \quad \text{(B5)}$$

$$D^S_{23}(P_k) = \left(\frac{nc_{23} + nc_{44}}{r}\right)P_k, \; D^S_{24}(P_k) = -(c_{44})P_k, \quad \text{(B6)}$$

$$D^S_{31}(P_k) = (c_{13})P_{k,r} + \left(\frac{c_{23}}{r}\right)P_k,$$

$$D^S_{32}(P_k) = \left(\frac{nc_{23} + nc_{44}}{r}\right)P_k, \quad \text{(B7)}$$

$$D^S_{33}(P_k) = -\left(\frac{n^2c_{44}}{r^2}\right)P_k, \; D^S_{34}(P_k) = -(c_{33})P_k, \quad \text{(B8)}$$

$$D^G_{11}(P_k) = (2n)P_k, \; D^G_{12}(P_k) = -(r)P_{k,r} - (2)P_k,$$
$$D^G_{13}(P_k) = -(n)P_{k,r} + \left(\frac{n}{r}\right)P_k, \quad \text{(B9)}$$

$$D^G_{21}(P_k) = (1)P_k, \; D^G_{22}(P_k) = (n)P_k,$$
$$D^G_{23}(P_k) = -(1)P_{k,r} + \left(\frac{n^2}{r}\right)P_k, \quad \text{(B10)}$$

$$D^G_{31}(P_k) = 0, \; D^G_{32}(P_k) = (r)P_k, \; D^G_{33}(P_k) = (n)P_k, \quad \text{(B11)}$$

and K_{ij} are

$$K_{11}(P_k) = (c_{11})P_{k,r} + \left(\frac{c_{12}}{r}\right)P_k, \; K_{12}(P_k) = \left(\frac{nc_{12}}{r}\right)P_k, \; K_{13}(P_k) = (c_{13})P_k, \quad \text{(B12)}$$

$$K_{21}(P_k) = \left(\frac{nc_{66}}{r}\right)P_k, \; K_{22}(P_k) = (c_{66})P_{k,r} - \left(\frac{c_{66}}{r}\right)P_k,$$

$$K_{23}(P_k) = 0, \quad \text{(B13)}$$

$$K_{31}(P_k) = (c_{55})P_k, \; K_{32}(P_k) = 0, \; K_{33}(P_k) = (c_{55})P_{k,r}. \quad \text{(B14)}$$